Research Article

Assessment of Low Linear Energy Transfer Radiation–Induced Bystander Mutagenesis in a Three-Dimensional Culture Model

Rudranath Persaud, Hongning Zhou, Sarah E. Baker, Tom K. Hei, and Eric J. Hall

Center for Radiological Research, Columbia University Medical Center, New York, New York

Abstract

A three-dimensional cell culture model composed of human-hamster hybrid (A_L) and Chinese hamster ovary (CHO) cells in multicellular clusters was used to investigate low linear energy transfer (LET) radiation–induced bystander genotoxicity. CHO cells were mixed with A_L cells in a 1:5 ratio and briefly centrifuged to produce a spheroid of 4×10^6 cells. CHO cells were labeled with tritiated thymidine ([^{3}H]dTTP) for 12 hours and subsequently incubated with A_L cells for 24 hours at 11°C. The short-range β-particles emitted by [^{3}H]dTTP result in self-irradiation of labeled CHO cells; thus, biological effects on neighboring A_L cells can be attributed to the bystander response. Nonlabeled bystander A_L cells were isolated from among labeled CHO cells by using a magnetic separation technique. Treatment of CHO cells with 100 μCi [^{3}H]dTTP resulted in a 14-fold increase in bystander mutation incidence among neighboring A_L cells compared with controls. Multiplex PCR analysis revealed the types of mutants to be significantly different from those of spontaneous origin. The free radical scavenger DMSO or the gap junction inhibitor Lindane within the clusters significantly reduced the mutation incidence. The use of A_L cells that are dominant negative for connexin 43 and lack gap junction formation produced a complete attenuation of the bystander mutagenic response. These data provide evidence that low LET radiation can induce bystander mutagenesis in a three-dimensional model and that reactive oxygen species and intercellular communication may have a modulating role. The results of this study will address the relevant issues of actual target size and radiation quality and are likely to have a significant effect on our current understanding of radiation risk assessment. (Cancer Res 2005; 65(21): 9876-82)

Introduction

The radiation-induced "bystander effect" refers to the induction of biological effects in cells that are not directly traversed by a charged particle but are in close proximity to cells that are. The bystander effect has been shown for a variety of end points, such as micronucleus induction, cell lethality, gene expression, and oncogenic transformation, by using a range of rodent and human cell culture models, but most studies have involved high linear energy transfer (LET) α-particles (1). There is clearly a need to ascertain whether a similar response can be observed with low LET radiation at doses correlating to environmental exposure.

There is evidence that low LET radiation can induce a cytotoxic bystander response in mammalian cells (2, 3). By using DMSO and Lindane as modulators, Bishayee et al. (4, 5) have shown that bystander cytotoxicity is free radical initiated and gap junction mediated, respectively. Furthermore, there is evidence that damage to cells from short-range β-particles resulted in an enhanced transformation yield among cells in close proximity by a factor of 10 compared with cells not in contact with damaged cells (6). In addition, X-rays delivered by a microbeam that targeted a single cell in a population produced bystander cell cytotoxicity that was similar to that when all the cells were exposed (7). Studies have also investigated the direct effects of low LET radiation where the entire population of cells was targeted and subsequently evaluated. Low LET protons were found to produce cytotoxicity, micronuclei induction, CD59 mutations, hypoxanthine phosphoribosyltransferase mutations, and chromosomal aberrations (8–11).

Evidence for a bystander response based on in vivo studies are rather limited. By evaluating tumor growth in mice, a significant growth inhibitory effect was observed within the nonirradiated, bystander tumor cell population adjacent to neighboring ^{3}H-labeled tumor cells emitting short-range β-particles (12). By using exogenous neutron-irradiated bone marrow cells implanted in mice, the progeny was determined to exhibit chromosomal instability (13). The present study uses a heterogeneous three-dimensional multicellular model that can mimic a tissue microenvironment and thereby provide important information on the relevance of the bystander effect to in vivo conditions.

Many bystander studies with low LET radiation involve the analysis of the cells as one population and not separately as directly labeled/irradiated compared with the unlabeled/nonirradiated bystander cells. This study separated and isolated the directly labeled Chinese hamster ovary (CHO) cells from the neighboring nonlabeled bystander A_L cells within the clusters. This allows for the most effective evaluation of the bystander response because the bystander A_L cell population can be studied independently for cytotoxicity and mutagenesis. The human-hamster hybrid A_L cells used in this study contain a full set of hamster chromosomes and a single copy of human chromosome 11, which includes the CD59 gene that encodes for the CD59 cell surface antigen. Mutants (CD59$^-$) can be detected and scored with the use of a complement-mediated cytotoxicity assay that uses the E7.1 monoclonal antibody against the CD59 antigen to destroy wild-type CD59$^+$ cells while sparing CD59$^-$ cells that subsequently proliferate to form mutant colonies. The mutation spectra of such mutants can be determined with great specificity because mutations are detectable that range in size from a single base pair to chromosomal mutations involving the loss of the entire human chromosome 11.

The demonstration of low LET radiation–induced bystander mutagenesis in a cell culture model that represents in vivo conditions may influence the calculations involved in risk assessment. This could subsequently result in changes in risk management for low LET radiation exposure. This study was undertaken to show

a correlation between low LET radiation and bystander mutagenicity in a three-dimensional cell culture model and to implicate the roles of reactive oxygen species and gap junctional intercellular communication in the bystander response.

Materials and Methods

Cell culture. For this study, human-hamster hybrid (A_L) and CHO cells were used. The A_L cells contain a standard set of Chinese hamster ovary-K1 chromosomes and a single copy of human chromosome 11 (14). Human chromosome 11 encodes for the CD59 cell surface antigen, and both the chromosome and the antigen can be used effectively in the separation and identification of A_L cells in a mixture with other cell types. Cultures were maintained in Ham's F-12 medium supplemented with 8% heat-inactivated fetal bovine serum, 25 μg/mL gentamicin, and 2× normal glycine (2×10^{-4} mol/L) at 37°C in a humidified 5% CO_2 incubator.

Radiochemical labeling of Chinese hamster ovary cells and preparation of multicellular clusters with A_L cells. Both 8×10^5 A_L and 8×10^5 CHO cells were preconditioned in 1 mL medium in 17×100 mm Falcon polypropylene culture tubes on a rocker-roller and incubated for 3 hours. Subsequently, 1 mL medium containing tritiated thymidine ([^{3}H]dTTP; Perkin-Elmer, Boston, MA) was added to the tubes containing CHO cells to produce various activities of the radionuclide. Tubes with control CHO or A_L cells received 1 mL medium. All tubes were incubated for 12 hours after which they were washed thrice with medium to remove excess [^{3}H]dTTP from labeled CHO cells. Four tubes of unlabeled A_L cells were incorporated into one tube of radiolabeled CHO cells to produce a mixture with a total of 4×10^6 cells that resulted in a ratio of 1:5 of radiolabeled CHO cells to unlabeled A_L cells. The cell mixture was centrifuged to produce a pellet and transferred in 0.4 mL medium to a sterile 500 μL microcentrifuge tube. This tube was centrifuged at 1,000 rpm for 1 minute to produce a cluster.

Separation of A_L and Chinese hamster ovary cell clusters by magnetic cell separation. Clusters were maintained at 11°C for 24 hours to allow self-irradiation of CHO cells and possible traversal of any bystander signals to neighboring A_L cells. After exposure, the supernatant was carefully removed and discarded. The clusters were dispersed, transferred to 17×100 mm Falcon polypropylene culture tubes, and washed in PBS/EDTA buffer. The cell mixtures were treated for 30 minutes at 4°C with a primary CD59 antibody (Serotec, Inc., Raleigh, NC) that binds the cell surface antigen on A_L cells. Magnetic beads, coated with rabbit anti-mouse IgG that acts as a secondary antibody to the monoclonal CD59 antibody, were incorporated into the cell mixtures and incubated at 4°C for 15 minutes. The cell mixtures were then passed twice through separation columns between magnets (Miltenyi Biotec, Auburn, CA). The effluent contained the unbound CHO fractions, whereas the A_L portions remained in the columns. The columns were removed from between the magnets and the A_L cells were flushed with the aid of a plunger.

Flow cytometric analysis of the separated fractions of Chinese hamster ovary and A_L cells. After incubation of A_L and CHO cells in clusters, magnetic separation was used to isolate two independent populations. To establish whether the separation was proficient, analyses on various mixtures of A_L and CHO cells were done to determine the efficiency of the magnetic separation. This was achieved by using flow cytometric analysis that specifically identifies a FITC tag on the A_L cells. To prepare the cells for such analysis, FITC-conjugated microbeads, as secondary antibodies to the CD59 primary antibody, were used during the separation. The immunophenotypical quantification of A_L cells in each population was done with the use of a FACSCalibur flow cytometer (BD Biosciences, San Jose, CA).

Role of free radicals and intercellular communication. To investigate the role of free radicals, and cell-to-cell communication in bystander mutagenesis, the radical scavenger DMSO (J.T. Baker, Phillipsburg, NJ) and the gap junction inhibitor Lindane (Sigma Chemical Co., St. Louis, MO) were used, respectively. DMSO was used as a 0.2% mixture with medium, and Lindane was used at a concentration of 40 μmol/L. Before the

formation of multicellular clusters, cells were washed with medium containing either DMSO or Lindane and clusters were generated. To eliminate the indirect effects of Lindane, connexin 43–deficient A_L cells (DN6) that lack functional gap junctions were used in the cluster. Cells (CXV2) containing the empty vector were used as their controls.

Functional gap junction formation between Chinese hamster ovary and A_L cells. To show that intercellular communication was operational between A_L and CHO cells within the three-dimensional model, transfer of the dye Calcein M (Molecular Probes, Boston, MA) from CHO to A_L cells was determined. Briefly, 8×10^5 CHO cells were incubated with 20 μmol/L Calcein M for 25 minutes and washed twice with PBS to remove excess dye. The cells were resuspended in medium and incubated for 30 minutes. Control and nondyed cells were treated the same. CHO cells were combined with 3.2×10^6 A_L cells, centrifuged to produce a cluster, and incubated for 24 hours at 11°C. This temperature was chosen to reduce the metabolic rate of the cells, thereby allowing them to survive in the spheroid formation. The cluster was resuspended in fluorescence-activated cell sorting buffer and the extent of dye migration was determined by a FACSCalibur flow cytometer.

Dose response for cell cytotoxicity. After the magnetic separation of the clusters into A_L and CHO fractions, cells were counted by using a hemocytometer and then plated into 100 mm diameter Petri dishes for colony formation. Cultures were incubated for 7 days, after which they were fixed with formaldehyde and stained with Giemsa. The number of colonies was counted to determine the survival fraction.

Determination of the mutant frequency. To determine bystander mutation, 2×10^5 cells were plated evenly on 12 single-well chamber slides, resulting in ∼16,666 cells per slide and incubated for 2 hours to allow for cell attachment. After incubation, 0.3% CD59 antiserum and 1.5% (v/v) rabbit serum complement (Covance, Denver, PA) were added as described (15). The slides were incubated for 7 days to allow for mutant colony formation. A_L cells become sensitive to the CD59 antibody in the presence of complement leading to lyses. However, A_L cells that are mutated at the CD59 marker become resistant and proliferate to form colonies.

Quantification of bystander mutants. Because the separation of A_L and CHO cells by magnetic cell separation may not be entirely efficient, it was necessary to differentiate between the two types of colonies by implementing immunofluorescent staining of human chromosome 11 present in A_L cells. The chamber slides with colonies were fixed, probed for human chromosome 11 by fluorescent *in situ* hybridization (FISH) using a peptide nucleic acid (Applied Biosystems, Farmingham, MA) targeted toward the centromeres as described (16). However, mutants that may have lost the entire centromere would not be detected. Positive A_L colonies were scored with the use of a confocal microscope. The mutant fraction at each dose was calculated as the number of surviving mutant colonies divided by the product of the total number of cells plated and the plating efficiency due to the presence of complement alone.

PCR analysis of mutant spectrum. Mutants were independently generated in 30×10–mm dishes and two mutants were isolated from each dish. The colonies were expanded in T-25 flasks, had their DNA extracted, and PCR analysis done as described (17, 18). Five marker genes on human chromosome 11 (Wilms' tumor, parathyroid hormone, catalase, RAS, and apolipoprotein A-1) were subjected to PCR analysis based on their mapping positions relative to the *CD59* gene. Amplifications were done for 30 cycles by using a DNA thermal cycler model 480 (Perkin-Elmer/Cetus) in a 20 μL reaction mixture containing 0.2 μg DNA sample in 1× Stoffel fragment buffer, the four deoxynucleotide triphosphates, 3 mmol/L $MgCl_2$, 0.2 mmol/L of each primer, and 2 units Stoffel fragment enzyme. The PCR reaction cycle was composed of denaturation at 94°C for 1 minute, annealing at 55°C for 1 minute, and extension at 72°C for 1 minute. The PCR products were electrophoresed on 3% agarose gels and stained with ethidium bromide.

Statistical analysis. Data for cytotoxicity and mutation were calculated as means and SDs of such means. Statistical significance of survival fractions and mutant fractions was determined by the Student's t test. $P \leq 0.05$ between groups was considered to be statistically significant.

Results

Efficiency of the magnetic separation of A_L and Chinese hamster ovary cells. This study is primarily focused on the bystander response among neighboring A_L cells adjacent to directly labeled CHO cells. To evaluate biological responses only in the bystander A_L cells, the two cell types were segregated by a magnetic cell separation technique. The competence of such a technique was confirmed by using flow cytometric analysis of the two cell populations. When 20% of CHO cells were mixed with 80% of A_L cells containing the human chromosome 11 encoded CD59 surface antigens, the latter was purified by using magnetic beads coated with FITC-conjugated secondary antibodies that bind to the A_L cells. Figure 1 depicts the results of the A_L fraction after magnetic bead purification (Fig. 1*C*) and subjected to flow cytometric analysis. The purity of the A_L fraction was determined to be 99.24%. The controls were unstained CHO (Fig. 1*A*) and unstained A_L (Fig. 1*B*) cells.

Activity of ^{3}H in A_L and Chinese hamster ovary cell populations after magnetic separation. It is critical that [^{3}H]dTTP from directly labeled CHO cells does not enter the bystander A_L
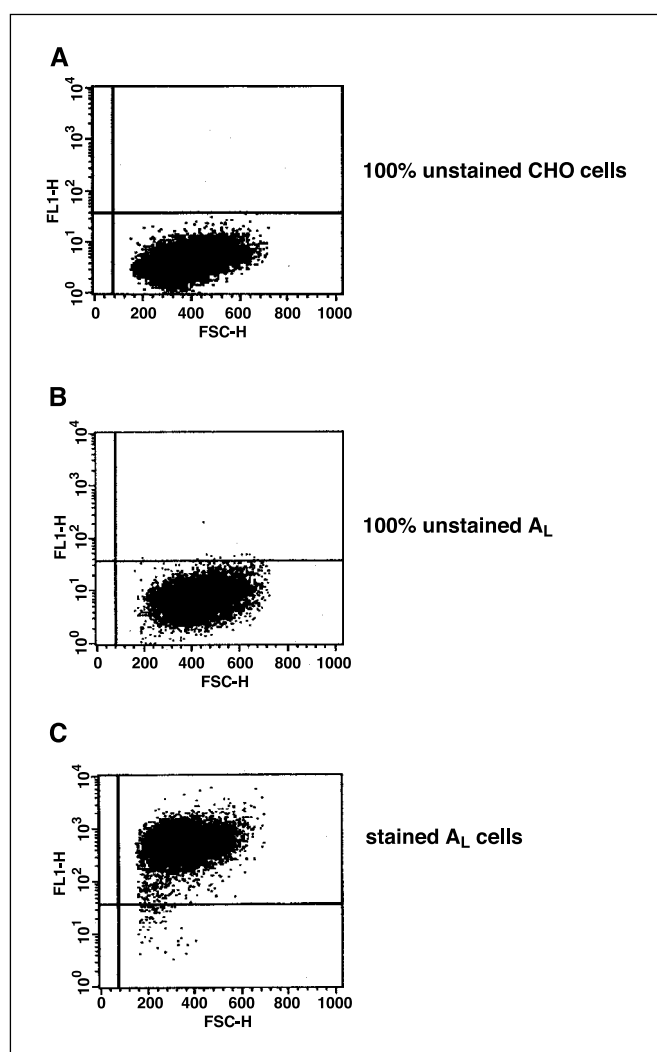

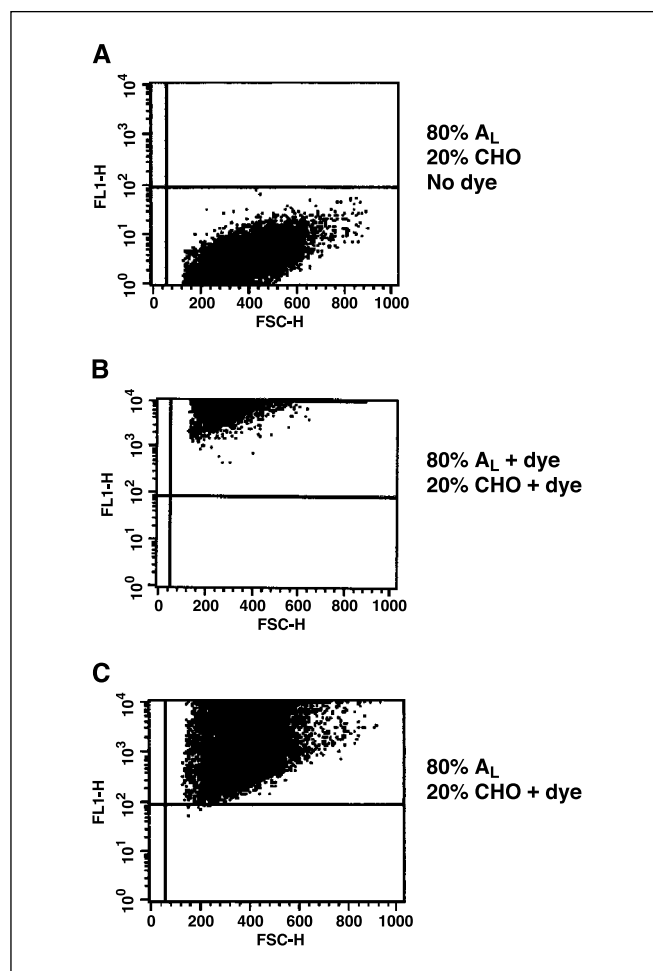**Figure 2.** Flow cytometric analysis to show the formation of functional gap junctions between A_L and CHO cells in cluster. *A,* 80% nondyed A_L and 20% nondyed CHO cells. *B,* 100% dyed A_L and CHO cells. *C,* 20% dyed CHO cells cocultured with 80% nondyed A_L cells.

cells within the cluster. The direct labeling of A_L cells can result in an exacerbation of the bystander cytotoxicity and mutagenesis. To establish that there was no incorporation of radioactivity into bystander A_L cells, the ^{3}H activity of the cell populations was measured after magnetic separation. The directly labeled CHO cell fraction had radioactivity of 2,250,850 cpm, whereas that of the bystander A_L population was only 6,775 cpm or 0.3% that of the CHO cells.

Gap junctional intercellular communication between Chinese hamster ovary and A_L cells in cluster. The transfer of the dye Calcein M was used to establish the formation of gap junctions between cells of the mixed population. Once taken up by CHO cells, the dye can only traverse to neighboring A_L cells through such junctions (5). As indicated by Fig. 2, when only the CHO cell population was exposed to Calcein M with subsequent coculturing with A_L cells in a cluster, 100% of the cell population, including the A_L cells, acquired the dye as shown in Fig. 2*C*. Figure 2*A* shows control, nondyed CHO, and nondyed A_L cells, and Fig. 2*B* shows 100% dyed cells.

Cytotoxicity of Chinese hamster ovary and bystander A_L cells in cluster. Figure 3 shows the dose-response relationship for clonogenic survival of previously directly labeled CHO cells and

Figure 1. Flow cytometric analysis of clusters of A_L/CHO cells after magnetic separation. Each cluster is composed of 20% CHO and 80% A_L cells. *A* and *B,* 100% control unstained CHO and A_L cells, respectively. *C,* purity of the A_L cell fraction is 99.24% after separation from CHO cells.

nonlabeled neighboring bystander A_L cells after 24 hours of coculture in a cluster where the ratio of CHO-to-A_L cells was 1:5. The clusters consisted of 4×10^6 cells of which 8×10^5 were CHO cells and 3.2×10^6 were A_L cells. At the highest dose of 100 µCi [^{3}H]dTTP, survival fractions for CHO and A_L cells were 0.37 ± 0.04 and 0.56 ± 0.05, respectively, corresponding to a significant difference ($P < 0.05$) in survival compared with their respective controls. It was obvious from these data that the nonirradiated cells showed a strong bystander effect in the mixed culture.

Mutagenicity of bystander A_L cells in cluster with Chinese hamster ovary cells exposed previously to 100 µCi [^{3}H]dTTP. The bystander A_L cells were cultured for 7 days to allow for clonal expansion and expression, after which they were analyzed for mutagenesis. As shown in Fig. 4A, when 80% of A_L cells were mixed with 20% of nonlabeled CHO cells, the background CD59$^-$ mutants were $\sim 20 \pm 15$ mutants per 10^5 survivors. In contrast, the CD59$^-$ mutant fraction increased to 270 ± 53 mutants per 10^5 survivors when A_L cells were mixed with 20% of labeled CHO cells, an increase of 14-fold ($P < 0.05$) above background.

Mutant spectrum analysis. Multiplex PCR was used to determine the types of mutations associated with the CD59$^-$ phenotype in the bystander A_L cells. Individual clones were isolated and analyzed for five human chromosome 11 markers located on either side of the *CD59* gene. A total of 190 mutants were analyzed, including 41 of spontaneous origin. As shown in Fig. 4B, 59% of the spontaneous CD59$^-$ mutants retained all of the markers. By contrast, 80% of the bystander CD59$^-$ mutants serving as bystanders to CHO cells directly labeled with 100 µCi [^{3}H]dTTP had lost at least one additional marker. This included 44% that lost a minimum of three additional markers. These data indicated that deletion mutations occur at a higher frequency in bystander CD59$^-$ mutants from clusters with 20% of ^{3}H-labeled CHO cells than in clusters with nonlabeled CHO cells.

Role of reactive oxygen species in bystander mutagenesis. To determine whether reactive oxygen species contribute to bystander mutagenesis resulting from low LET exposure, the radical scavenger DMSO was incorporated into the clusters. As shown in
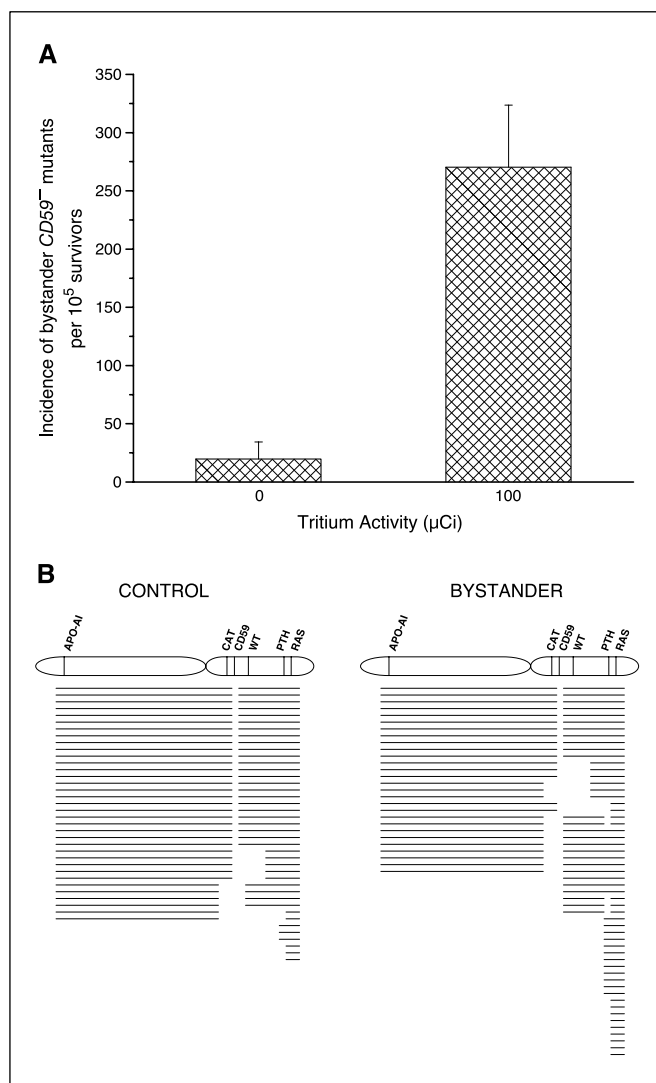

Figure 4. *A,* incidence of bystander CD59$^-$ mutants among A_L cells clustered with CHO cells that were either labeled with 100 µCi [^{3}H]dTTP or no labeling. *Columns,* mean of four experiments; *bars,* SD. *B,* mutant spectrum of bystander CD59$^-$ mutants among A_L cells clustered with CHO cells that were either labeled with 100 µCi [^{3}H]dTTP or no labeling.
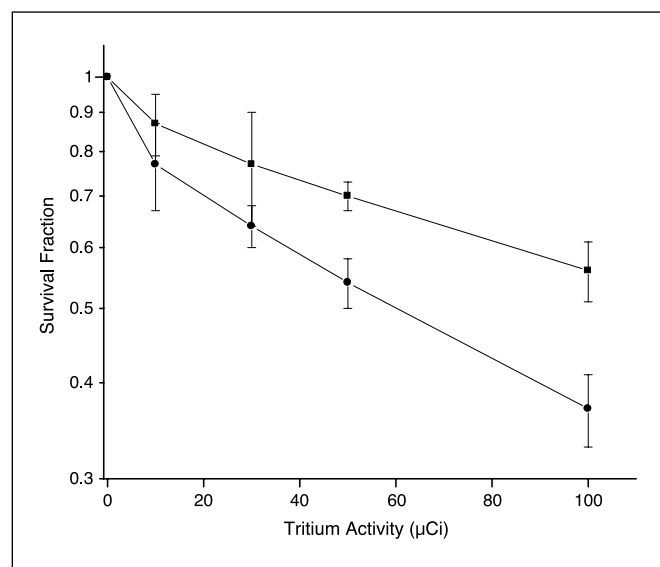

Figure 3. Survival of bystander A_L cells (■) in cluster with CHO cells (●) labeled with graded doses of [^{3}H]dTTP. *Points,* mean of three to four experiments; *bars,* SD.

Fig. 5, 0.2% DMSO was not cytotoxic and nonmutagenic to the A_L cells because the survival fraction and the mutant fraction were almost identical to that of control. When DMSO was incorporated into the cells in the cluster and maintained throughout the incubation period, the bystander mutation frequency was reduced from 118 ± 30 per 10^5 survivors to 63 ± 12 per 10^5 survivors, corresponding to a 50% reduction. These data indicated that free radicals, mainly hydroxyl radicals, may participate in the pathway leading to bystander mutagenesis.

Role of cell-to-cell communication in bystander mutagenesis. Previous studies from this laboratory and others have shown that Lindane can inhibit cell-to-cell communication (19–21). To evaluate the contribution of cell-to-cell communication between directly labeled CHO cells and neighboring nonlabeled bystander A_L cells, experiments were conducted by using Lindane, an inhibitor of gap junctional intercellular communication, within the cluster. Figure 6 shows that Lindane was able to significantly decrease the mutant fraction from 174 ± 26 per 10^5 survivors to

84 ± 17 per 10^5 survivors, representing a 52% reduction in mutant fraction. In addition, using connexin 43–deficient A_L cells resulted in a reduction of the bystander mutant fraction from 291 ± 17 per 10^5 survivors to 17 ± 4 per 10^5 survivors, representing a complete attenuation (Fig. 7).

Discussion

This study used a three-dimensional multicellular cluster, with two cell types, CHO and A_L, which were separated after incubation and analyzed as two independent cell populations, the directly labeled versus bystander populations, respectively. There were five times more A_L cells than CHO cells in the cluster. The CHO cells were directly labeled with [^{3}H]dTTP that was incorporated into their DNA, and A_L cells served as bystanders. The mean energy of β-particles emitted from ^{3}H is only 5.7 keV. This is equivalent to a range of only 1 μm in water (22). Because the diameter of a CHO cell nucleus is roughly 7 to 8 μm, nearly all the cells will be self-irradiated with little probability that the β-particles will be able to exit the CHO nucleus and hit neighboring, bystander A_L cells in the cluster. To ensure that A_L bystanders were not directly labeled by [^{3}H]dTTP, two separate approaches were undertaken. First, labeled CHO cells were washed thoroughly to remove any trace of extracellular radioactivity before mixing with the A_L cells. After the final centrifugation to establish the cell clusters, the supernatants were recovered and found to have minimum radioactivity. Second, after the magnetic separation, the radioactivity of the enriched A_L cell population was determined to be 0.3% of the directly labeled CHO cells. This level of activity can be attributed to the few directly labeled CHO cells that may be present in the A_L cell fraction because the efficiency of separation was found to be only 99.24%. Another concern is the possibility of tritium release from CHO cells undergoing apoptosis. However, CHO cell DNA fragments from the apoptotic process are too large to cross the cell membrane and be taken up by A_L cells. Therefore, it implies that any detrimental effects detected among bystander A_L cells will most certainly result from signals originating in directly labeled CHO cells. Bystander A_L cells can respond to mediators from CHO cells because they are
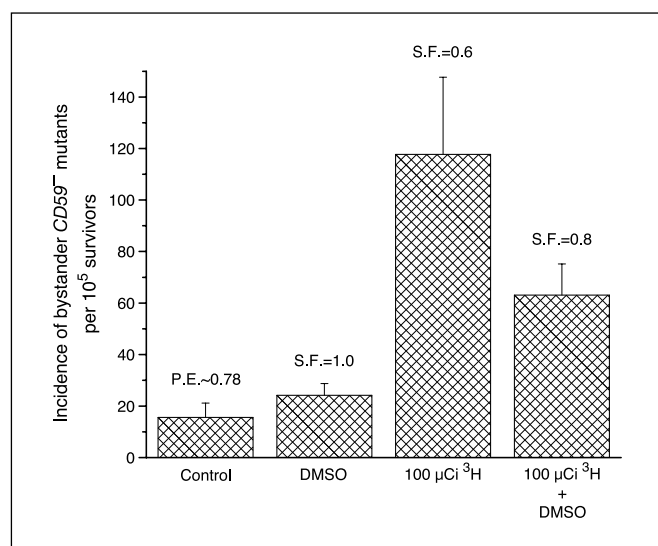

Figure 6. Effect of Lindane (40 μmol/L) on the incidence of bystander CD59⁻ mutants among A_L cells in cluster with CHO cells exposed previously to 100 μCi [^{3}H]dTTP. *Columns,* mean of three experiments; *bars,* SD.
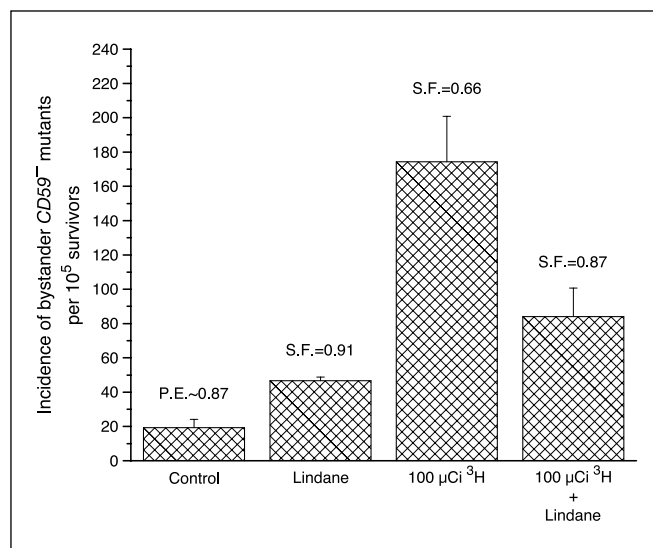
CHO cells in lineage, although A_L cells contain a single copy of human chromosome 11.

The direct labeling of a target population of cells and subsequent incorporation of nonlabeled cells is another approach toward investigating the low LET radiation–induced bystander phenomenon. The other commonly used techniques involved medium-mediated experiments (2, 23) and targeted approaches, such as microbeams (8, 9), where the radiation insult is temporary and the irradiated and nonirradiated cells are analyzed together. In the present study, the incorporation of ^{3}H into the DNA of directly labeled CHO cells will emit β-particles that deposit their energy therein throughout the 24-hour incubation period. For the other techniques, the initial insult lasts only a few seconds; thus, any bystander response produced by nonirradiated cells depends mainly on mediators released into the environment and/or a traversal of signals through gap junctions between targeted and nontargeted cells. For diagnostic or therapeutic purposes, exposure to low LET radiation is relatively short term; thus, any bystander response will propagate from the initial interaction with the impending radiation as can be shown *in vitro* by medium-mediated bystander experiments. However, in terms of occupational or environmental exposure, the duration is usually long term and becomes more significant if the radionuclide enters the biological system. The present work will, therefore, provide significant insight into occupational or environmental exposure, such as that associated with Department of Energy cleanup operations and space travel.

Previous bystander studies with β-particles have shown cell lethality as the major end point of the bystander effect (3–5). The present study is the first to report that mutagenesis, as well as cell lethality, occurs in neighboring bystander A_L cells clustered with directly labeled CHO cells. Because the observed incidence of mutation was a measurement of changes on the single copy of human chromosome 11 present in the human-hamster hybrid A_L cells, it was probable that mutational changes were also imparted to the hamster genome in the hybrid A_L cells and may have contributed to cytotoxicity. The 0.56 survival fraction observed for bystander A_L cells was equated with a 14-fold increase in bystander
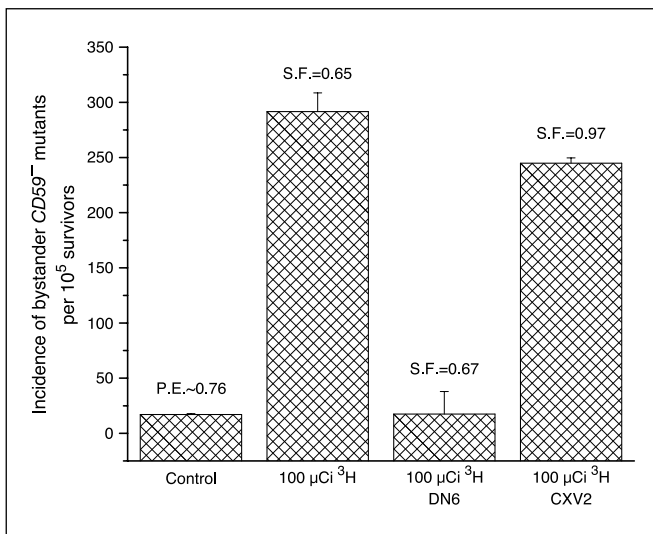

Figure 5. Effect of DMSO (0.2%) on the incidence of bystander CD59⁻ mutants among A_L cells in cluster with CHO cells exposed previously to 100 μCi [^{3}H]dTTP. *Columns,* mean of three experiments; *bars,* SD.

Figure 7. Incidence of bystander CD59⁻ mutants among connexin 43–deficient A$_L$ cells (*DN6*) and empty vector-transfected A$_L$ cells (*CXV2*) clustered with CHO cells that were either labeled with 100 μCi [³H]dTTP or no labeling. *Columns,* mean of three experiments; *bars,* SD.

mutation incidence. A 10-fold transformation yield was observed previously in neighboring cells in proximity to cells also exposed to β-particles (6). The background mutation incidence of 20 ± 15 mutants per 10^5 survivors was relatively lower than reported previously (20). This can be attributed to the magnetic separation technique used to partition the clusters into the A$_L$ and CHO fractions. This procedure uses affinity binding of an antibody toward the CD59 cell surface antigen on A$_L$ cells. Only CD59⁺ A$_L$ cells will be immobilized on the separation column and become available for the CD59 antibody-complement mutation assay. In addition, CHO cells present in the bystander A$_L$ fraction after magnetic separation can proliferate and be mistaken for mutant colonies. To score only A$_L$ mutant colonies, the centromeres of the human chromosome 11 in the cells were probed by a peptide nucleic acid using FISH. The sequence of the probe is complementary to that of centromeres found in human chromosomes only. This implies there will be no cross-reactivity with hamster chromosomes; thus, only A$_L$ mutant colonies will be stained and scored. However, mutants that have lost the entire centromeric region will not be scored leading to an underestimation of the mutant fraction. CD59-deficient cells that are lacking the centromere can arise following exposure to sparsely ionizing radiation (24); thus, it is likely that the procedures used for mutant selection in the present study underestimate the true CD59 mutant fraction. This limitation may also induce bias toward the observed mutant spectra for both control and treated cultures depending on the proportion of mutants that have lost the centromeric region. Nevertheless, the underestimated mutant yield will not change the observed bystander mutagenic yield or the conclusions drawn. Furthermore, a partial loss of the centromere will not affect the efficiency of detection as the probe does not require the complete sequence of bases.

The significant increase in cell lethality and mutation incidence indicated a potent bystander signal or a significant amplification of the bystander response especially because there were five times more bystander A$_L$. The three-dimensional cluster conformation provides more effective interaction of mediators because there is more contact between the cell types compared with a two-dimensional model. The cluster model also prevents any considerable dilution of secreted mediators. The mutation spectra obtained for the bystander A$_L$ cells was able to complement the observed mutation incidence. A significant number of multilocus deletions were observed in the majority of clones. Similar spectra were generated from direct exposure of A$_L$ cells to X-rays and A$_L$ cells to nitrogen and proton ions that target the entire population of cells (10, 24). The overlap of mutation spectra implies that similar mediators may be responsible for mutagenesis arising from the bystander response or direct exposure to low LET radiation. It must be noted that the reduction in metabolic activity as a consequence of incubation at 11°C may influence the magnitude of the bystander signals and counter response.

The β-particles emitted from ³H incorporated into the DNA of targeted CHO cells deposit energy that may ionize water molecules in the vicinity leading to the initiation of lipid peroxidation, a probable initial event. The data obtained from the utilization of DMSO suggest that reactive oxygen species, mainly hydroxyl radicals, a potent initiator of lipid peroxidation, may be involved in the early stages of the cascade sequence. Bishayee et al. (5) provided evidence to support this finding with low LET radiation by using ³H in a multicellular cluster with cell lethality as the end point. However, with high LET α-particles, DMSO did not inhibit the bystander mutagenic response in nonirradiated neighboring cells (20). These observations suggest that the type of radiation may influence the mediators and pathways involved in the bystander response.

The cluster of CHO and A$_L$ cells allows for intimate contact between the different types of cells. The migration of the fluorescent dye Calcein M from dyed CHO cells to nondyed A$_L$ cells justified the formation of functional gap junctions allowing for intercellular communication. The present finding that Lindane provides protection against the low LET radiation–induced bystander response is consistent with these observations. To further confirm the role of intercellular communication, A$_L$ cells, dominant negative for connexin 43 that will impair gap junction formation, were used to evaluate bystander mutagenesis. In such cells, there was complete attenuation of the bystander mutagenic response.

The actual mediator or signal that influences neighboring bystander A$_L$ cells to elicit responses remains to be identified. The size of molecules that can traverse gap junctions is usually <1,500 Da (25) and can include a myriad of ions and small molecules. The reactive oxygen species that may be generated by the ionization of water are short-lived and can only migrate distances significantly smaller than the diameter of cells; thus, oxyradicals are unlikely to be directly responsible for the bystander effect. It is plausible that the generation of reactive oxygen species is among the preliminary events that occur in CHO cells incorporating ³H. This can subsequently lead to the synthesis and/or secretion of molecules, small peptide mediators, or sequestered ions into the intercellular space or through gap junctions. Secretion of such might lead to interaction with the membrane or intracellular components of neighboring bystander A$_L$ cells possibly leading to the initiation of a second messenger system. Because the cells are in clusters for 24 hours with continuous insult, this may result in the synthesis of secondary mediators that are not normally present in any significant concentrations. From medium-mediated and microbeam experiments where the irradiation time is <1 minute, it suggests that the

initial reaction to the stress is enough to propel the targeted cells to produce bystander mediators.

The present study provides evidence that low LET radiation from directly labeled cells can illicit a mutagenic response in neighboring bystander cells and suggests that a signaling pathway involving reactive oxygen species and/or the secretion of mediator molecules may contribute to the observed bystander effect. Because free radicals are unlikely to traverse cells, it is possible that secreted mediators can induce reactive oxygen species formation in bystander A_L cells that can contribute to cytotoxicity and mutagenesis. The numerous multilocus deletions observed in the mutant colonies suggest that such oxyradicals may be directly involved in the mutation event. The possible utilization of gap junctions for the transmission and propagation of the bystander signal to adjacent cells implies that it requires a relatively small number of target cells to elicit a major response. The bystander cytotoxicity and mutagenesis findings of this study are consistent with those from high LET radiation studies with α-particles. Therefore, it implies that risk assessment for low LET radiation exposure may require similar management guidelines as those established for high LET radiation.

Acknowledgments

References

1. Hall EJ, Hei TK. Genomic instability and bystander effects induced by high-LET radiation. Oncogene 2003; 22:7034–42.
2. Mothersill C, Seymour CB. Medium from irradiated human epithelial cells but not human fibroblasts reduces the clonogenic survival of unirradiated cells. Int J Radiat Biol 1997;71:421–7.
3. Bishayee A, Rao DV, Howell RW. Evidence for pronounced bystander effects caused by nonuniform distributions of radioactivity using a novel three-dimensional tissue culture model. Radiat Res 1999;152: 88–97.
4. Bishayee A, Rao DV, Bouchet LG, Bolch WE, Howell RW. Protection by DMSO against cell death caused by intracellularly localized iodine-125, iodine-131 and polonium-210. Radiat Res 2000;153:416–27.
5. Bishayee A, Hill HZ, Stein D, Rao DV, Howell RW. Free radical-initiated and gap junction-mediated bystander effect due to nonuniform distribution of incorporated radioactivity in a three-dimensional tissue culture model. Radiat Res 2001;155:335–44.
6. Sigg M, Crompton NEA, Burhart W. Enhanced neoplastic transformation in an inhomogeneous radiation field: an effect of the presence of heavily damaged cells. Radiat Res 1997;148:543–7.
7. Schettino G, Folkard M, Prise KM, Voynovic B, Held KD, Michael BD. Low-dose studies of bystander cell killing with targeted soft X rays. Radiat Res 2003;160: 505–11.
8. Schettino G, Folkard M, Prise KM, Voynovic B, Bowey AG, Michael BD. Low-dose hypersensitivity in Chinese hamster V79 cells targeted with counted protons using a charged-particle microbeam. Radiat Res 2001;156:525–34.
9. Prise KM, Folkard M, Malcolmson AM, et al. Single ion actions: the induction of micronuclei in V79 cells exposed to individual protons. Adv Space Res 2000;25: 2095–101.
10. Wedemeyer N, Greve B, Uthe D, et al. Frequency of CD59 mutations induced in human-hamster hybrid A_L cells by low-dose X-irradiation. Mutat Res 2001;473: 73–84.
11. Mognato M, Bortoletto E, Ferraro P, et al. Genetic damage induced by *in vitro* irradiation of human G_0 lymphocytes with low-energy protons (28 keV/μm): HPRT mutations and chromosomal aberrations. Radiat Res 2003;160:52–60.
12. Xue LY, Butler NJ, Makrigiorgos GM, Adelstein SJ, Kassis AI. Bystander effect produced by radiolabeled tumor cells *in vivo*. Proc Natl Acad Sci U S A 2002;99: 13765–70.
13. Watson GE, Lorimore SA, Macdonald DA, Wright EG. Chromosomal instability in unirradiated cells induced *in vivo* by a bystander effect of ionizing radiation. Cancer Res 2000;60:5608–11.
14. Waldren CA, Jones C, Puck TT. Measurement of mutagenesis in mammalian cells. Proc Natl Acad Sci U S A 1979;76:1358–62.
15. Zu L, Waldren CA, Vannais D, Hei TK. Cellular and molecular analysis of mutagenesis induced by charged particles of defined LET. Radiat Res 1996;145:251–9.
16. Williams B, Stender H, Coull JM. PNA fluorescent *in situ* hybridization for rapid microbiology and cytogenetic analysis. In: Nielsen PE, editor. Peptide nucleic acids: methods and protocols. Totowa (NJ): Humana Press; 2002. p. 181–93.
17. Hei TK, Wu LJ, Liu SX, Vannais D, Waldren CA, Randers-Pehrson G. Mutagenic effects of a single and exact number of α particles in mammalian cells. Proc Natl Acad Sci U S A 1997;94:3765–70.
18. Hei TK, Piao CQ, He ZY, Vannais D, Waldren CA. Chrysotile fiber is a potent mutagen in mammalian cells. Cancer Res 1992;52:6305–9.
19. Azzam EI, de Toledo SM, Gooding T, Little JB. Intercellular communication is involved in the bystander regulation of gene expression in human cells exposed to very low fluences of α particles. Radiat Res 1998;150: 497–504.
20. Zhou H, Randers-Pehrson G, Waldren CA, Vannais D, Hall EJ, Hei TK. Induction of a bystander mutagenic effect of α particles in mammalian cells. Proc Natl Acad Sci U S A 2000;97:2099–104.
21. Shao C, Furusawa Y, Aoki M, Ando K. Role of gap junctional intercellular communication in radiation-induced bystander effect in human fibroblasts. Radiat Res 2003;160:318–23.
22. ICRU Publication 37. Stopping powers for electrons and positrons. Bethesda (MD): International Commission on Radiation Units and Measurements; 1984.
23. Shao C, Aoki M, Furusawa Y. Medium-mediated bystander effects on HSG cells co-cultivated with cells irradiated by X-rays or a 290 MeV/μ carbon beam. J Radiat Res 2001;42:305–16.
24. Kraemer SM, Kronenberg A, Ueno A, Waldren CA. Measuring the spectrum of mutation induced by the human-hamster hybrid cell line A_LC. Radiat Res 2000; 153:743–51.
25. Prise KM, Folkard M, Michael BD. Bystander responses induced by low LET radiation. Oncogene 2003;22:7043–9.